Rational ab initio modeling for polytypic transformations and phase stability in kaolin materials

Mercier, Patrick H. J.; Le Page, Yvon

https://doi.org/10.4224/21085173

RATIONAL AB INITIO MODELING FOR POLYTYPIC TRANSFORMATIONS AND PHASE STABILITY IN KAOLIN MINERALS

Patrick H.J. Mercier*, Yvon Le Page

National Research Council of Canada, NRC Energy, Mining and Environment Portfolio, 1200 Montreal Road, Ottawa, Ontario, Canada

Presented at:
American Crystallographic Association Annual Meeting
Boston, MA, USA
July 26–August 1, 2012

*patrick.mercier@nrc-cnrc.gc.ca

National Research Council Canada | Conseil national de recherches Canada

Canada

Topics for the lecture

Part 1

Concepts:
- Geometrically distinguishable stackings of 2 kaolin layers (Newnham 1962)
- Energy independence of non-adjacent layers
- Energy distinguishable low-energy structures (Mercier & Le Page 2008)
- No layer rotation upon solid state transformation (Dera et al. 2003)

Part 2

Model generation and ab initio quantum optimization

Part 3

Zero-pressure results
- Low energy / low enthalpy
- H vs P graph for kaolin polytypes
- Diagenetic interpretation

Part 4

Kaolin under high pressure (HP)
- New translations and HP phases predicted (Mercier & Le Page 2009)
- New HP polytypes observed (Welch & Crichton 2010)
- More HP polytypes predicted (Mercier, Le Page & Desgreniers 2010)

Part 5

ConcIn: When experiment is stalled, inexpensive theory can
- sift through "*known facts*"
- produce experimentally verifiable/falsifiable predictions

Progress acceleration

(Mercier & Le Page 2011)

Problem

Kaolin minerals are extremely abundant
and technologically important

but still

our knowledge of this system is an accumulation
of facts with many unanswered questions.

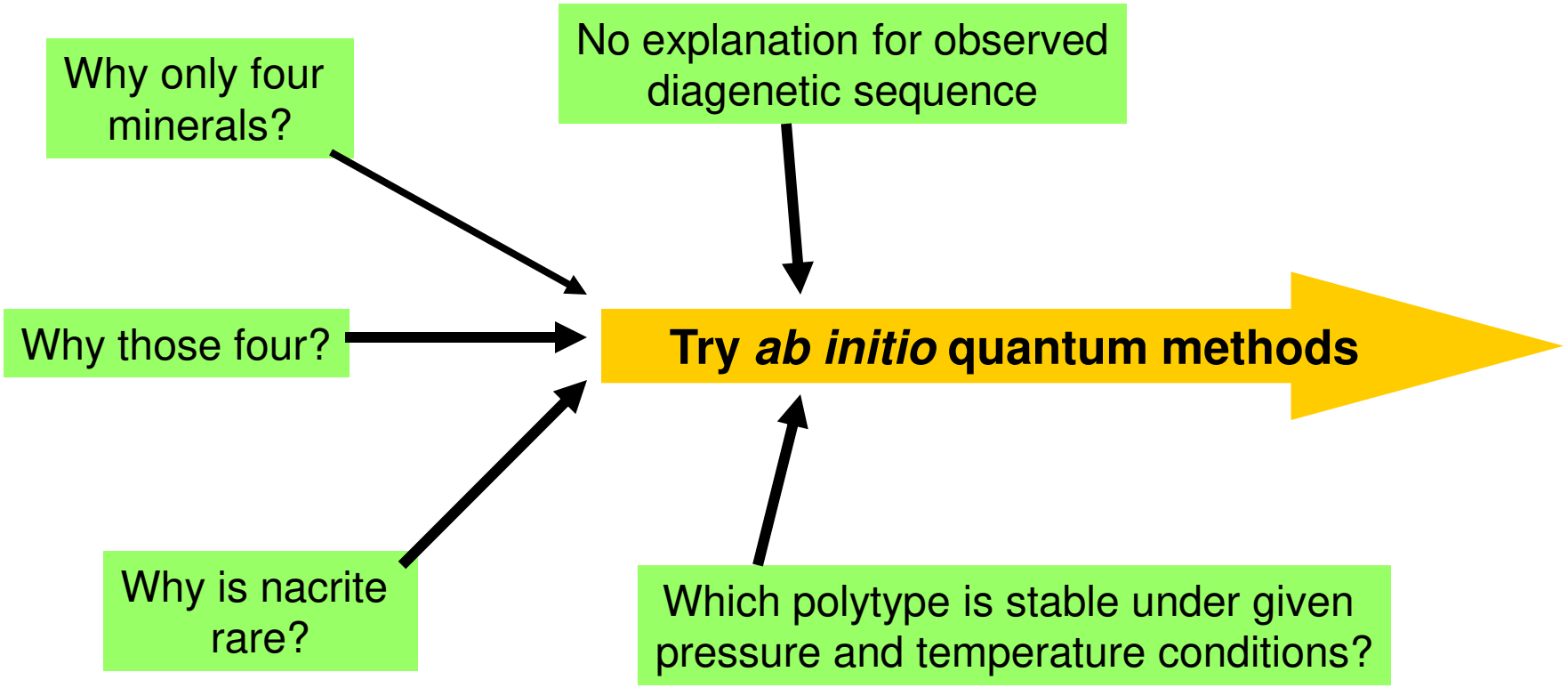

The lizardite layer, $Mg_3Si_2O_5(OH)_4$

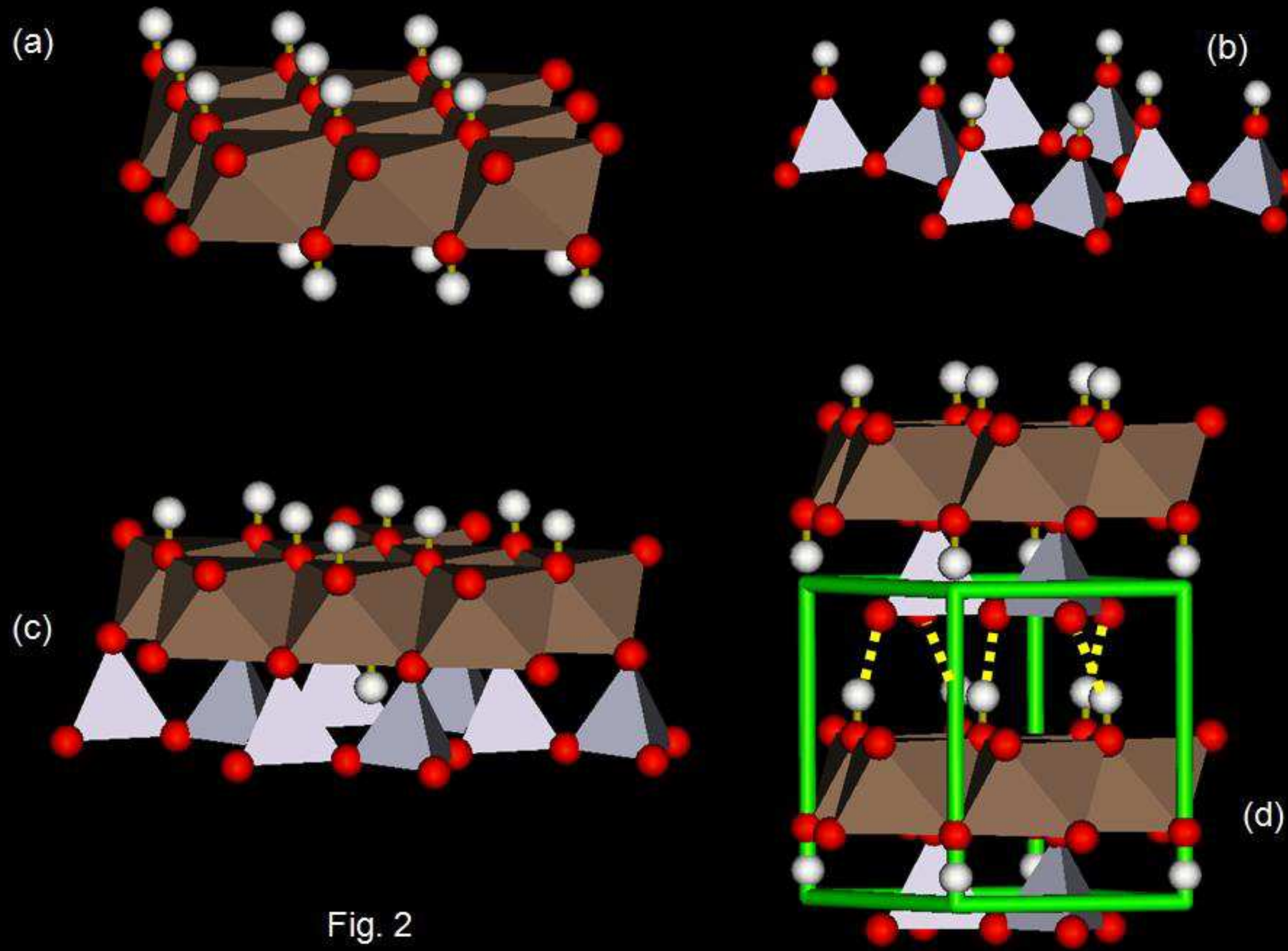

Fig. 2

Stacking lizardite layers

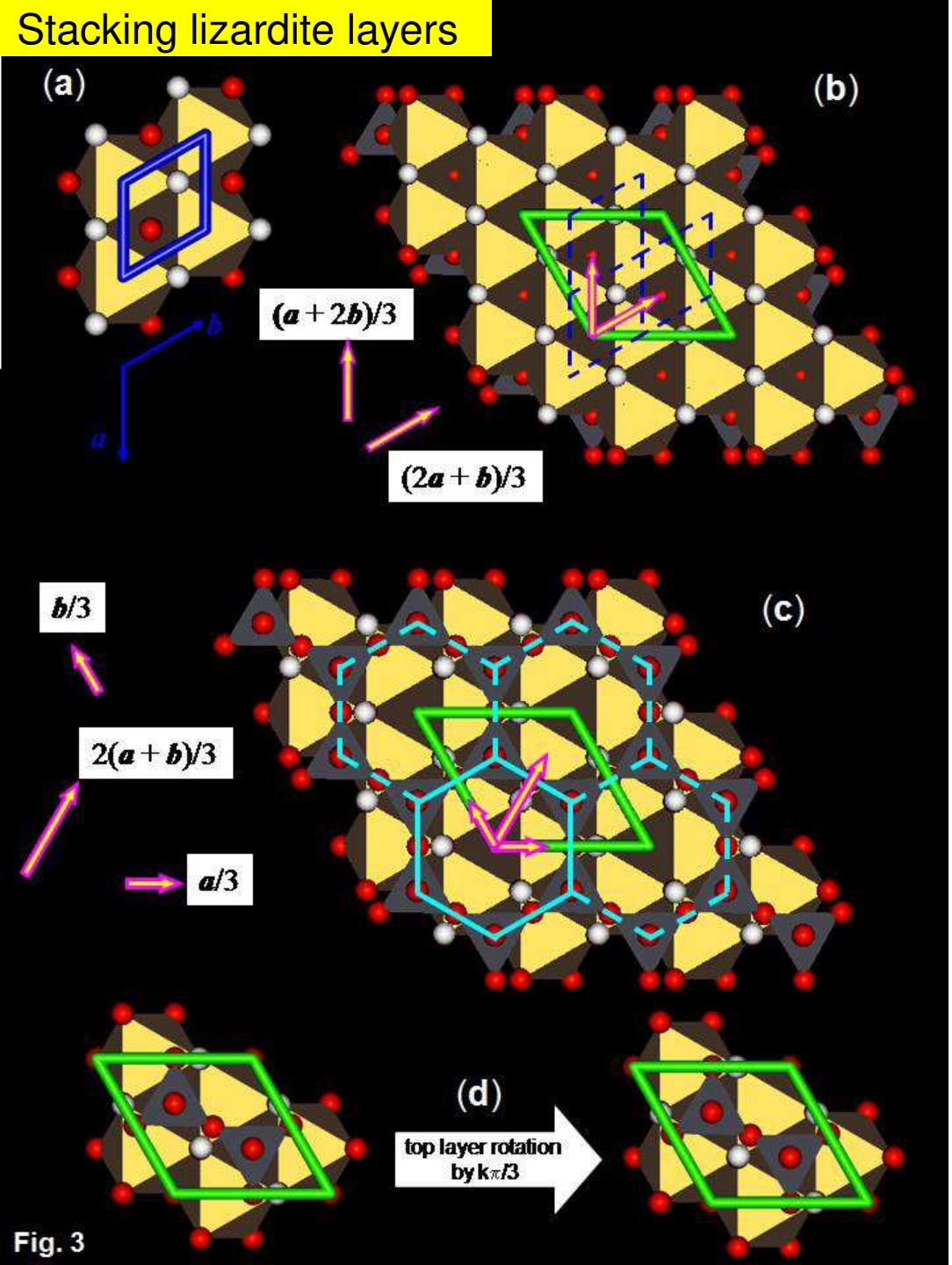

Fig. 3

Different stackings of lizardite layers are possible and distinguishable for the following reasons:

(i) Translations (2***a*** + ***b***)/3 and (***a*** + 2***b***)/3 repeat the brucite sheet (Fig. 3a) in the lizardite reference system (Fig. 3b). Under such displacement of the top lizardite layer, the same set of hydrogen bonds is then formed between the silicate and brucite sheets of adjacent layers, whereas silicate networks superpose differently.

(ii) Translations of the top layer by ***a***/3, ***b***/3 or 2(***a***+***b***)/3 (but not -***a***/3 etc.) shifts the centre of the silicate rings of the top layer from the vertical through the center of an anion triangle of the brucite layer pointing along -***a*** to the vertical of the centre of a triangular face of Mg-octahedra pointing along +***a***. As the silicate layer has approximate sixfold symmetry through the centre of the silicate rings, sets of hydrogen bonds analogous to those in (i) above can then form (Fig. 3c), but the layer stacking itself is different.

(iii) A rotation by kπ/3 about the *z* axis of the top lizardite layer approximately (k odd) or exactly (k even) reproduces the silicate sheet of the top layer with quasi six-fold symmetry (Fig. 3d).

Distinguishable stackings of two lizardite layers

•Translations ***a***/3, ***b***/3 or 2(***a***+***b***)/3 are related by the 3-fold symmetry axis through the origin; although distinguishable from the 1*T* stacking, the stackings they generate are not distinguishable among themselves.

• Translations (2***a***+***b***)/3 and (***a***+2***b***)/3 are mirror-related; the stackings they produce are accordingly distinguishable from one-another.

• Rotations by zero, 2π/3 and 4π/3 are also symmetry-related and produce identical objects; same goes for rotation by π/3, π, and 5π/3.

trans'n \ rot'n	0	π
0	L1 (=1*T*)	L2
(2***a***+***b***)/3	L3	L4
(***a***+2***b***)/3	L3*	L4*
a/3	L5	L6

4 translations X 2 rotations = 8 distinguishable models

6 energy-distinguishable
+
2 enantiomorphic models

The ideal kaolin layer $Al_2Si_2O_5(OH)_4$

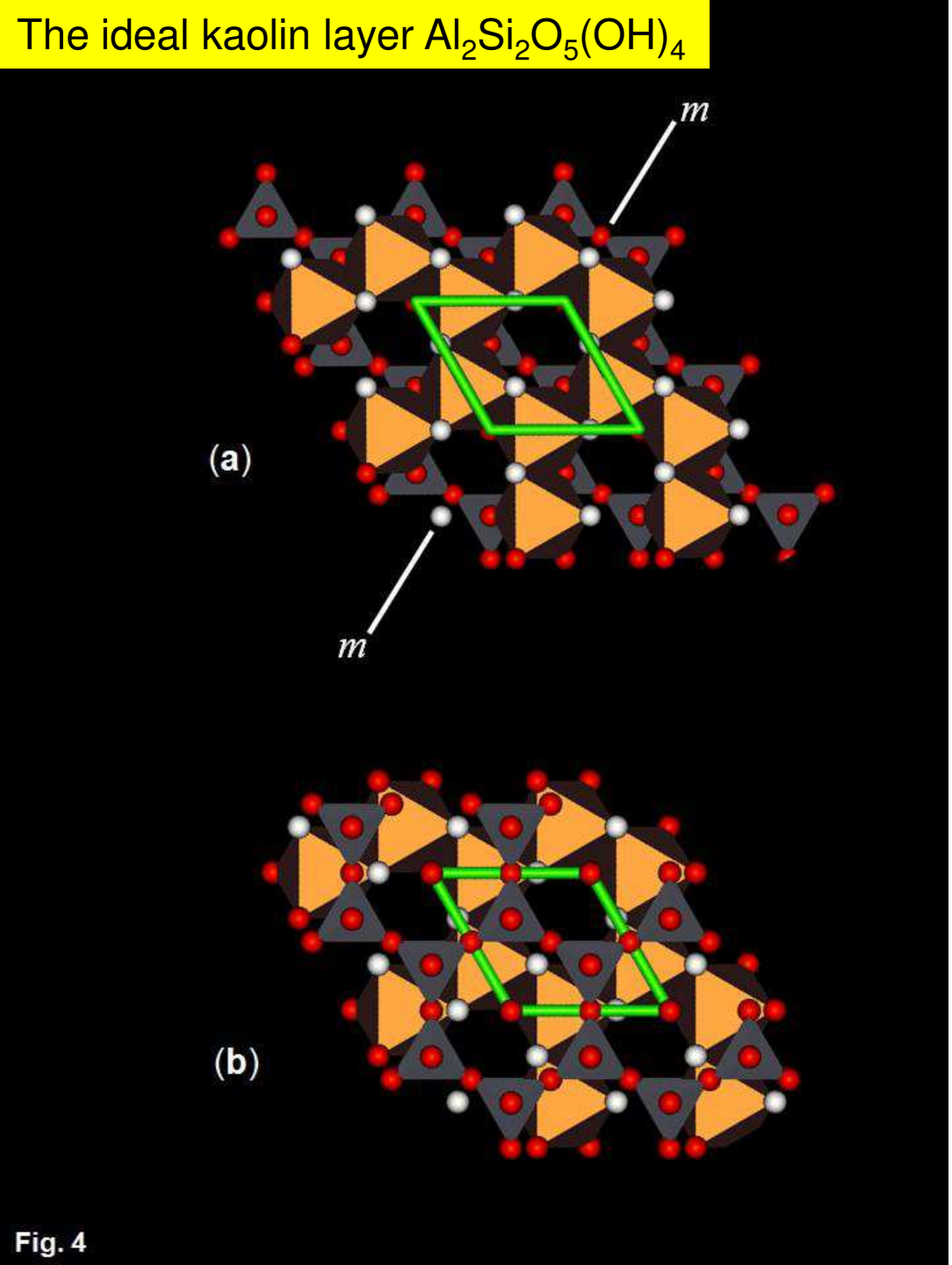

Fig. 4

The architecture of the kaolin layer derives from that of lizardite, $Mg_3Si_2O_5(OH)_4$, by replacing the three Mg^{2+} ions within the mesh by two Al^{3+} ions and a vacancy □.

This substitution destroys the threefold symmetry of lizardite and has been performed by replacing the Mg^{2+} atom at 2/3, 2/3, z along [110] in the lizardite mesh by a vacancy.

As a result, the point-group symmetry is reduced from 31*m* to *m*.

Ideal model of kaolin layer in space group P1

lizardite 1T

```
   cell
a=5.3267 Å
b=5.3267
c=7.2539
α= 90.000°
β= 90.000
γ=120.000
```

Si1	1(a)	0.333333333	0.666666667	0.137931035
Si2	1(a)	0.666666667	0.333333333	0.137931035
Al3	1(a)	0.333333333	0.000000000	0.515133834
Al4	1(a)	0.000000000	0.333333333	0.515133834
O5	1(a)	0.333333333	0.666666667	0.360050455
O6	1(a)	0.666666667	0.333333333	0.360050455
O7	1(a)	0.500000000	0.000000000	0.053885848
O8	1(a)	0.000000000	0.500000000	0.053885848
O9	1(a)	0.500000000	0.500000000	0.053885848
O10	1(a)	0.666666667	0.000000000	0.655209145
O11	1(a)	0.000000000	0.666666667	0.655209145
O12	1(a)	0.333333333	0.333333333	0.655209145
O13	1(a)	0.000000000	0.000000000	0.359049917
H14	1(a)	0.666666667	0.000000000	0.783278000
H15	1(a)	0.000000000	0.666666667	0.783278000
H16	1(a)	0.333333333	0.333333333	0.783278000
H17	1(a)	0.000000000	0.000000000	0.239985904

z coords from lizardite

x and y coordinates as multiples of sixths

From stackings of two kaolin layers to low-energy phases

Hydrogen bonding between layers allows:

Mercier & Le Page (2008)
Acta Cryst. B 64: 131-143

	0	2π/3	4π/3	π/3	π	5π/3
0	6 translations X 6 rotations					
(2***a***+***b***)/3						
(***a***+2***b***)/3	36 geometrically distinguishable **stackings of 2 layers** (Newnham, 1962)					
a/3	splitting into 20 [R,T] + 16 [-R,T*] energy distinguishable transformations, in turn giving					
b/3	**36 structure models** [RT]=[RT]= and [RT]=[-RT*]= as prime candidates for **low-energy phases**					
2(***a***+***b***)/3						

Energy independence for non-adjacent layers

Adjacent layers

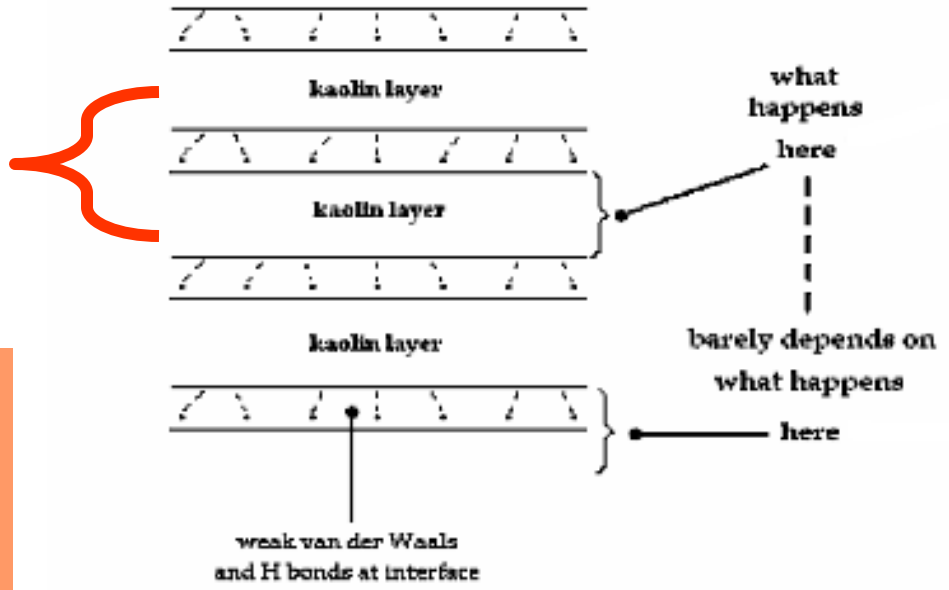

Total energy Utot is sum of energy for isolated kaolin layers plus corrections ΔA, ΔB, etc. for hydrogen bonding at single interfaces.

$$Utot = UA + UB + UC + \ldots = n\,U_{layer} + \Delta A + \Delta B + \Delta C + \ldots$$

As one of ΔA, ΔB, ΔC etc. is lower than all other ones, independence of non-adjacent layers implies that only transformations with that lowest energy ΔK are involved in the lowest-energy crystal stacking.

[(R,T)] repeated

[(R,T): (-R, T*)] repeated

Mercier & Le Page (2008) *Acta Cryst. B* 64: 131-143

Model creation

Possible lowest-energy polytypes now reduce to:

- Repeated application of (**R**, **T**) ➔ 20 models
- Application of (**R**, **T**) followed by (-**R**, **T***)
  ➔ 16 additional models

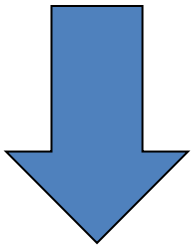

36 possible low-energy polytypes
(only 20 of those are in Newnham's 36)

2.1.2.

Repeated application of R and T

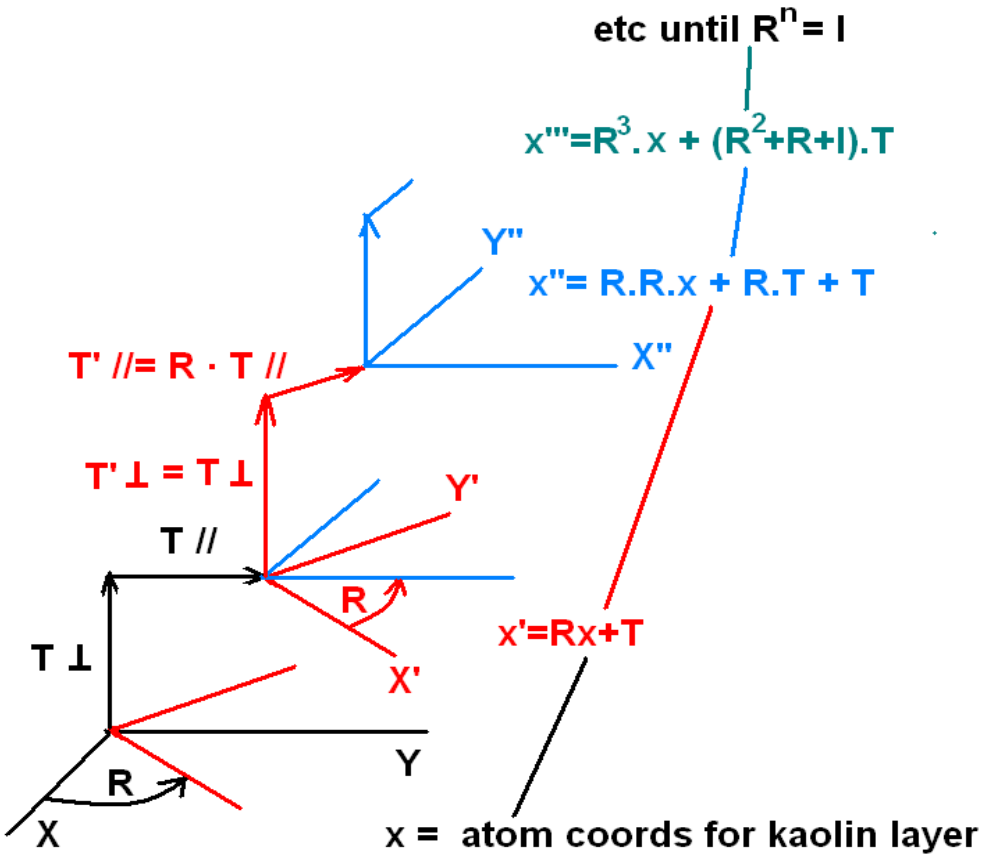

Vector $(R^{n-1} + R^{n-2} + ..+R+ I) \cdot T$ is then the ***c*** repeat of the generated stacking

2.1.3.

Application of (R,T), then (-R, T*)

The sum of the two rotations is zero
➔ only two layers.

Cell content is then x for layer 1
and R·x + T for layer 2.

Vector T + R·T*
is the ***c*** repeat of
the resulting model

Polytype Builder Tool operates on an ideal kaolin layer to create ideal polytype models with *Materials Toolkit*

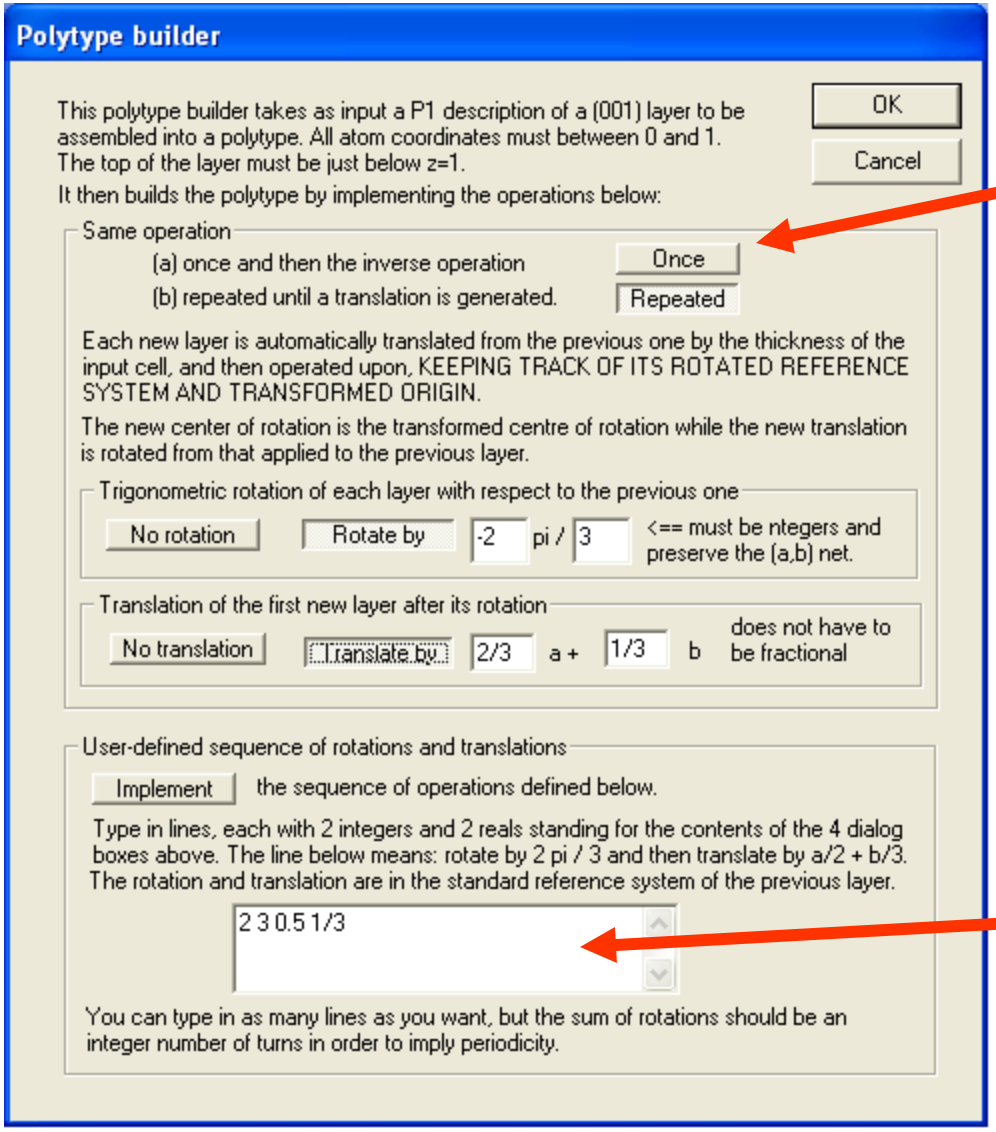

Sequence:
(R,T)
(-R,T*)

Repeated application of a same (R,T)

Any sequence of (R,T) operations with Σ (R) = 2kπ

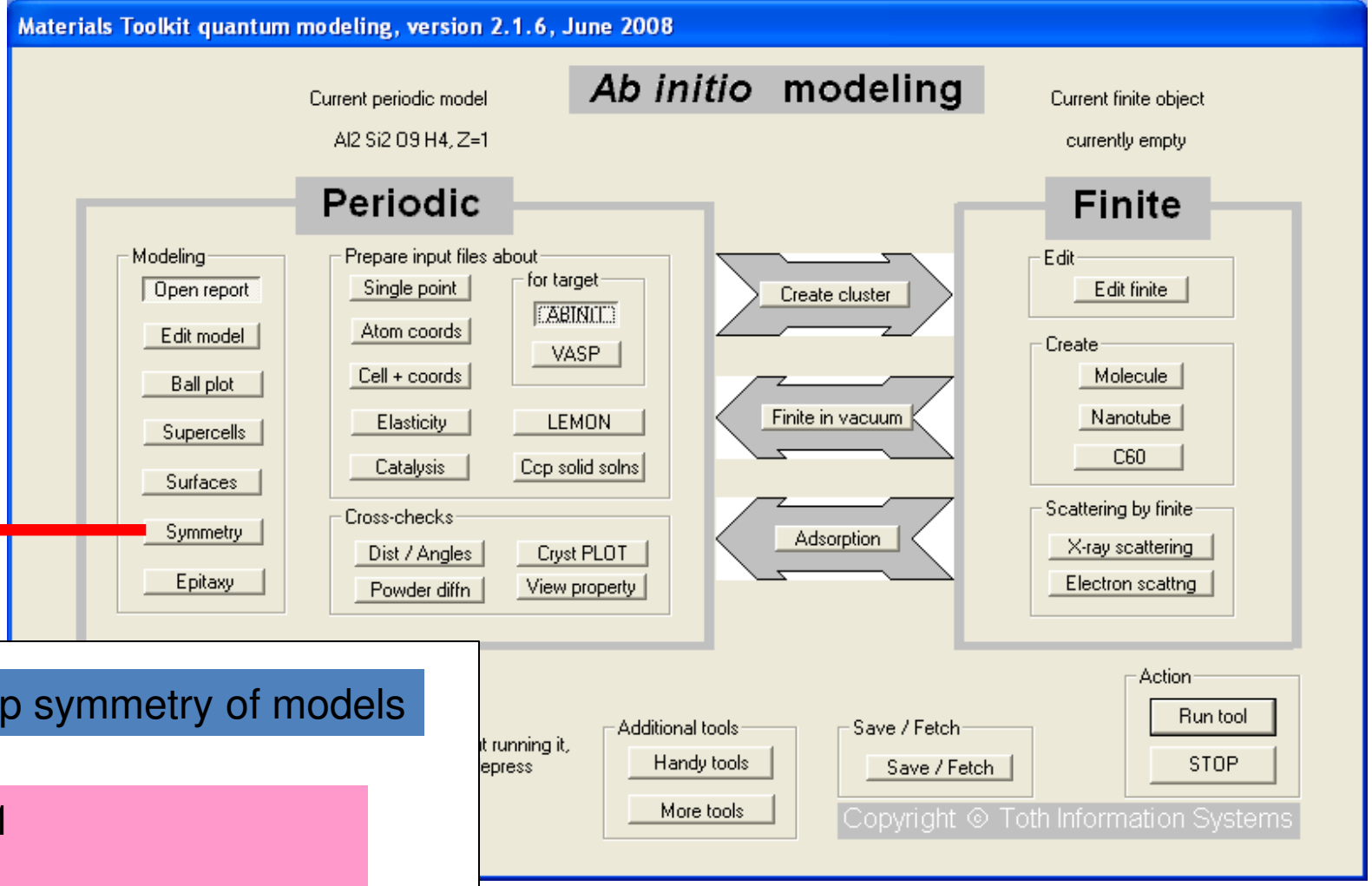

Space-group symmetry of models

1 layer: P1

2 layers $P2_1$, Cm, Cc, $Cmc2_1$

3 layers: $P3_1$

6 layers: $P6_1$

20 energy-distinguishable transformations
16 enantiomorphic transformations

	0	π/3	2π/3	π	4π/3	5π/3
0	K1	K2a	K3a	K4	K3a*	K2a*
(2***a***+***b***)/3	K5a	K6a	K7a	K8a	K10a*	K9a*
(***a***+2***b***)/3	K5a*	K9a	K10a	K8a*	K7a*	K6a*
a/3	K11a	K12a	K13a	K14a	K16a*	K15a*
b/3	K11a*	K15a	K16a	K14a*	K13a*	K12a*
2(***a***+***b***)/3	K17	K18a	K19a	K20	K19a*	K18a*

Mercier & Le Page (2008) *Acta Cryst. B* 64: 131-143

Kaolin polytypes revisited *ab initio*

Straightforward implementation of *ab initio* modeling with *Materials Toolkit* quantum interface

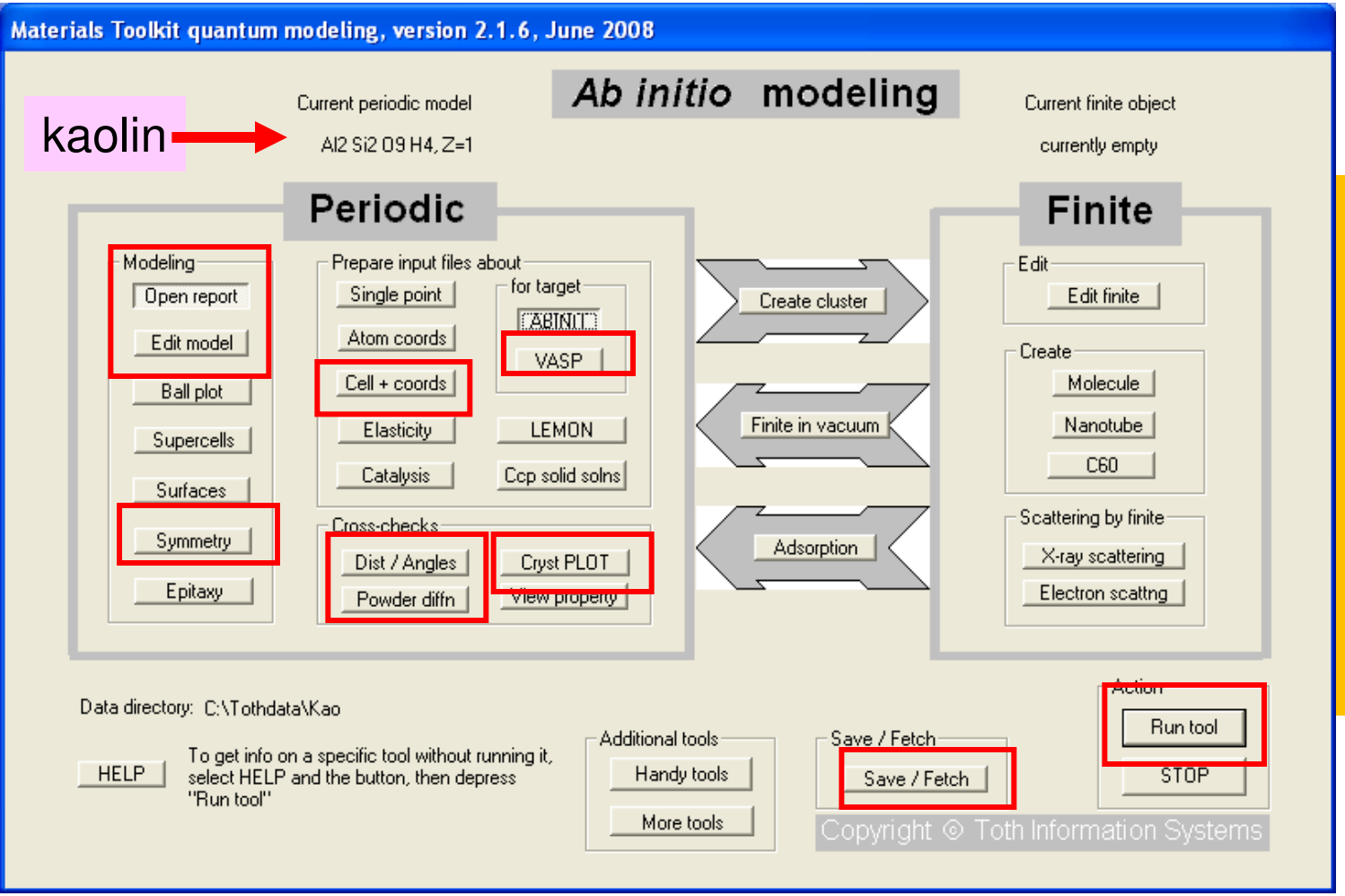

Quantum execution on Athlon Windows PCs: ~ 2 d each (2-layer models) up to ~ 2 weeks (6-layer models)

Le Page & Rodgers (2005) *J. Appl. Cryst.* 38: 697-705

Ab initio optimization of ideal models

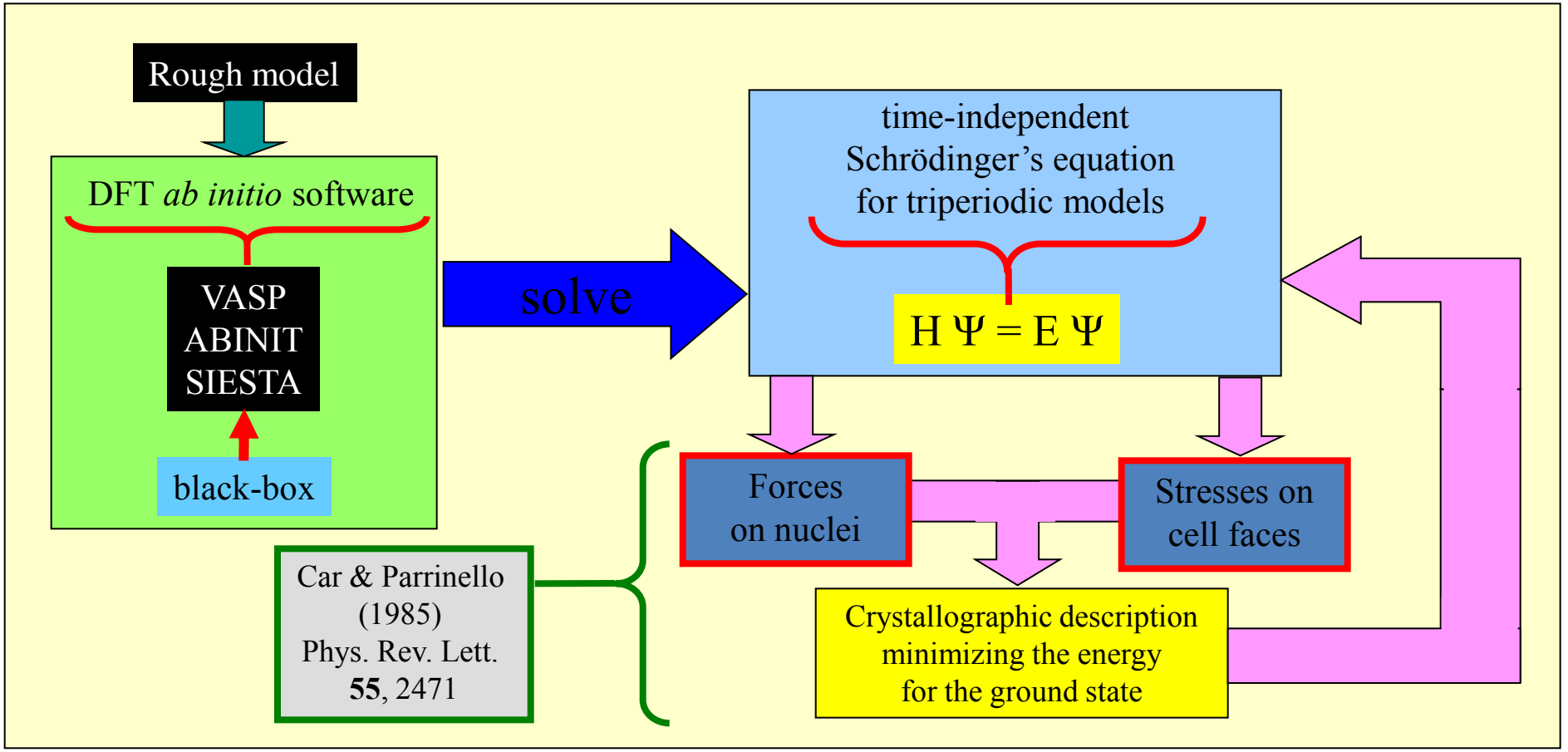

Blind optimization of 36 ideal models

derived starting from just
ideal topology of kaolin layers
and
basic scheme for interlayer H bonds

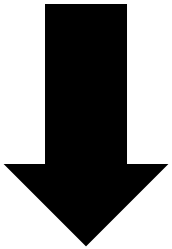

reproduces among the list
the
4 crystal forms of kaolin *then known*
including their
bond-lengths and bond-angle
distortions

Mercier & Le Page (2008) *Acta Cryst. B* 64: 131-143

Mercier & Le Page (2008)
***Acta Cryst. B* 64 : 131-143**

kaolinite-II

Welch & Crichton (2010) Am. Min. 95: 651-654

Blind optimization of 36 ideal models gives all four polytypes then known, including their distortions.

kaolinite

HP-dickite (dickite-II)

Dera et al. (2003) Am. Min. 88: 1428-1435

nacrite

dickite

Table 2
Low-energy stackings of two kaolin layers

Note: 1 meV per kaolin f.u. ≃ 0.0955 kJ mol^{-1}.

	Rotation					
	0	π/3	2π/3	π	4π/3	5π/3
(*a*) Repeated operations [*Kx*]						
Translation: 0						
Model No.	[K1]	[K2*a*]	[K3*a*]	[K4]	[K3*a*]*	[K2*a*]*
Space group	*Cm*	$P6_1$	$P3_1$	$Cmc2_1$	$P3_1$	$P6_5$
Free energy difference (meV per f.u.)	69	18	119	45	–	–
Volume difference (Å^3)	0.614	0.925	−1.081	0.459	–	–
Translation: (2a + b)/3						
Model No.	[K5*a*]	[K6*a*]	[K7*a*]	[K8*a*]	[K10*a*]*	[K9*a*]*
Space group	*P*1	$P6_1$	$P3_1$	$P2_1$	$P3_2$	$P6_5$
Free energy difference (meV per f.u.)	137	76	117	50	–	–
Volume difference (Å^3)	−2.863	0.433	−2.879	0.236	–	–
Translation: (a + 2b)/3						
Model No.	[K5*a*]*	[K9*a*]	[K10*a*]	[K8*a*]*	[K7*a*]*	[K6*a*]*
Space group	–	$P6_1$	$P3_1$	–	$P3_2$	$P6_5$
Free energy difference (meV per f.u.)	–	35	105	–	–	–
Volume difference (Å^3)	–	0.439	0.297	–	–	–
Translation: a/3						
Model No.	[K11*a*]	[K12*a*]	[K13*a*]	[K14*a*]	[K16*a*]*	[K15*a*]*
Space group	*P*1	$P6_1$	$P3_1$	$P2_1$	$P3_2$	$P6_5$
Free energy difference (meV per f.u.)	0	41	12	46	–	–
Volume difference (Å^3)	0.000	0.658	−0.085	−0.019	–	–
Translation: b/3						
Model No.	[K11*a*]*	[K15*a*]	[K16*a*]	[K14*a*]*	[K13*a*]*	[K12*a*]*
Space group	*P*1	$P6_1$	$P3_1$	$P2_1$	$P3_2$	$P6_5$
Free energy difference (meV per f.u.)	–	53	9	–	–	–
Volume difference (Å^3)	–	0.606	0.087	–	–	–
Translation: 2(a + b)/3						
Model No.	[K17]	[K18*a*]	[K19*a*]	[K20]	[K19*a*]*	[K18*a*]*
Space group	*Cm*	$P6_2$	$P3_1$	$Cmc2_1$	$P3_2$	$P6_4$
Free energy difference (meV per f.u.)	72	183	107	131	–	–
Volume difference (Å^3)	−1.430	−1.387	−1.468	−0.972	–	–
(*b*) Succession of operations [*Kx*] and then [*Kx*]*, the enantiomorph of [*Kx*]						
Translation: 0						
Model No.	–	[K2*b*]	[K3*b*]	–	[K3*b*]* = [K3*b*]	[K2*b*]* = [K2*b*]
Space group	–	*Cc*	*Cc*	–	*Cc*	*Cc*
Free energy difference (meV per f.u.)	–	29	106	–	–	–
Volume difference (Å^3)	–	0.438	−0.860	–	–	–
Translation: (2a + b)/3						
Model No.	[K5*b*]	[K6*b*]	[K7*b*]	[K8*b*]* = [K8*b*]	[K10*b*]* = [K10*b*]	[K9*b*]* = [K9*b*]
Space group	*Cc*	*Cc*	*Cc*	*Cc*	*Cc*	*Cc*
Free energy difference (meV per f.u.)	135	78	112	51	–	–
Volume difference (Å^3)	−0.796	−0.061	−2.843	0.250	–	–
Translation: (a + 2b)/3						
Model No.	[K5*b*]*	[K9*b*]	[K10*b*]	[K8*b*]* = [K8*b*]	[K7*b*]* = [K7*b*]	[K6*b*]* = [K6*b*]
Space group	*Cc*	*Cc*	*Cc*	*Cc*	*Cc*	*Cc*
Free energy difference (meV per f.u.)	–	59	132	–	–	–
Volume difference (Å^3)	–	−2.179	−0.826	–	–	–
Translation: a/3						
Model No.	[K11*b*]	[K12*b*]	[K13*b*]	[K14*b*]* = [K14*b*]	[K16*b*]* = [K16*b*]	[K15*b*]* = [K15*b*]
Space group	*Cc*	*Cc*	*Cc*	*Cc*	*Cc*	*Cc*
Free energy difference (meV per f.u.)	14	32	8	24	–	–
Volume difference (Å^3)	0.189	0.367	0.046	1.016	–	–
Translation: b/3						
Model No.	[K11*b*]*	[K15*b*]	[K16*b*]	[K14*b*]* = [K14*b*]	[K13*b*]* = [K13*b*]	[K12*b*]* = [K12*b*]
Space group	*Cc*	*Cc*	*Cc*	*Cc*	*Cc*	*Cc*
Free energy difference (meV per f.u.)	–	32	2	–	–	–
Volume difference (Å^3)	–	0.321	0.208	–	–	–
Translation: 2(a + b)/3						
Model No.	–	[K18*b*]	[K19*b*]	–	[K19*b*]* = [K19*b*]	[K18*b*]* = [K18*b*]
Space group	–	*Cc*	*Cc*	–	*Cc*	*Cc*
Free energy difference (meV per f.u.)	–	182	112	–	–	–
Volume difference (Å^3)	–	−1.350	−1.706	–	–	–

Other main observations

- Lowest energy is for kaolinite
- Next lowest energy is for dickite
- Half-a-dozen solutions with competitive energy
- Nacrite and HP-dickite are NOT among the very low energy solutions
- Highest energy is 183 meV (~18kJ/f.u.) higher than kaolinite

Mercier & Le Page (2008) *Acta Cryst. B* 64: 131-143

r.m.s. value
of calculated energy difference
between the
16 analogous EDT and EDT:EDT* stackings

~13 meV = ~1.2 kJ/mol
per formula unit
(~ ½ $k_B T$)

wide occurrence of stacking disorder in kaolin samples

energy contribution due to non-adjacent layers interactions

ab initio energy calculation error

both capped to ≈ 13 meV

Mercier & Le Page (2008)
Acta Cryst. B 64: 131-143

Free Energy *versus* Enthalpy

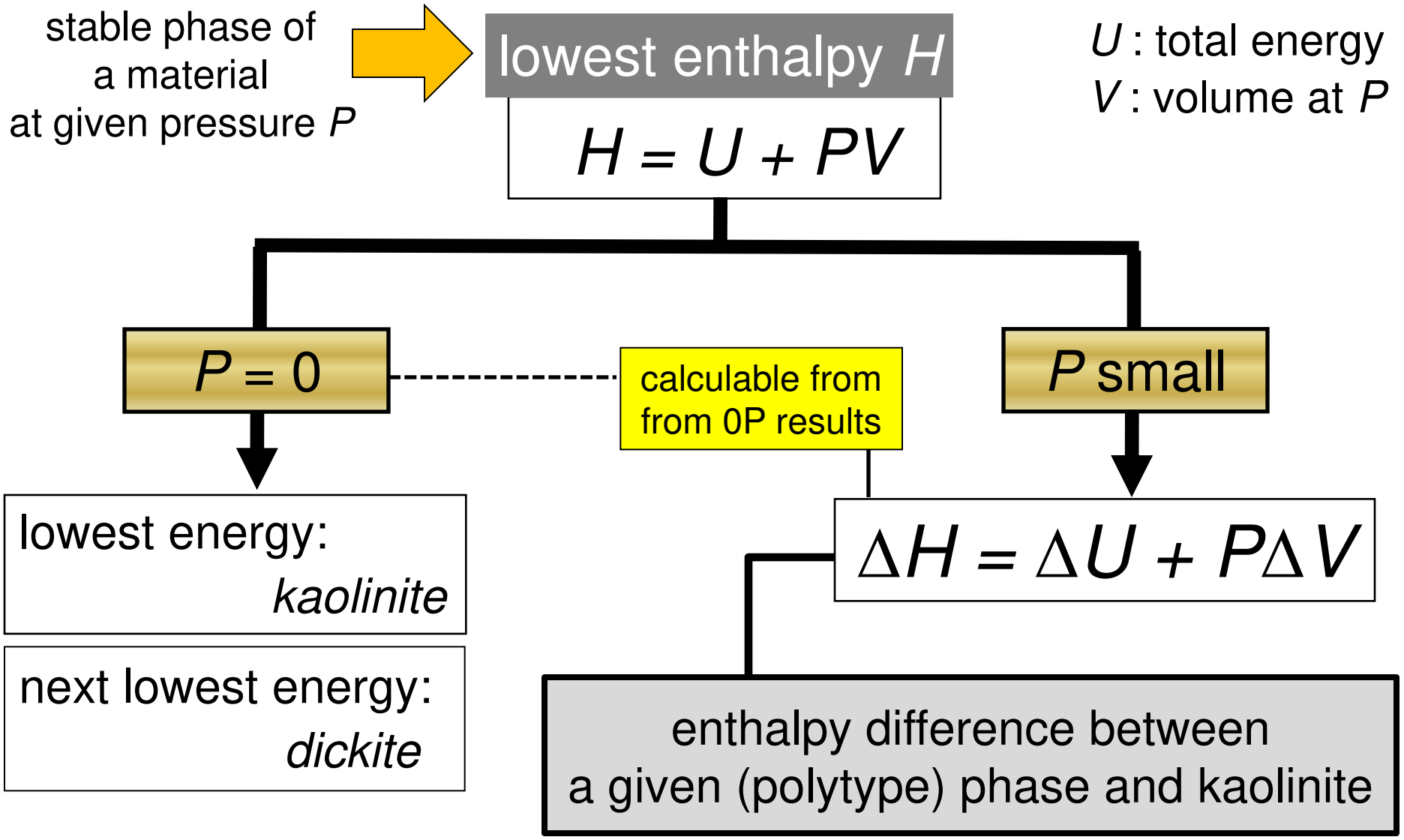

Stability of kaolin polytypes at 0K

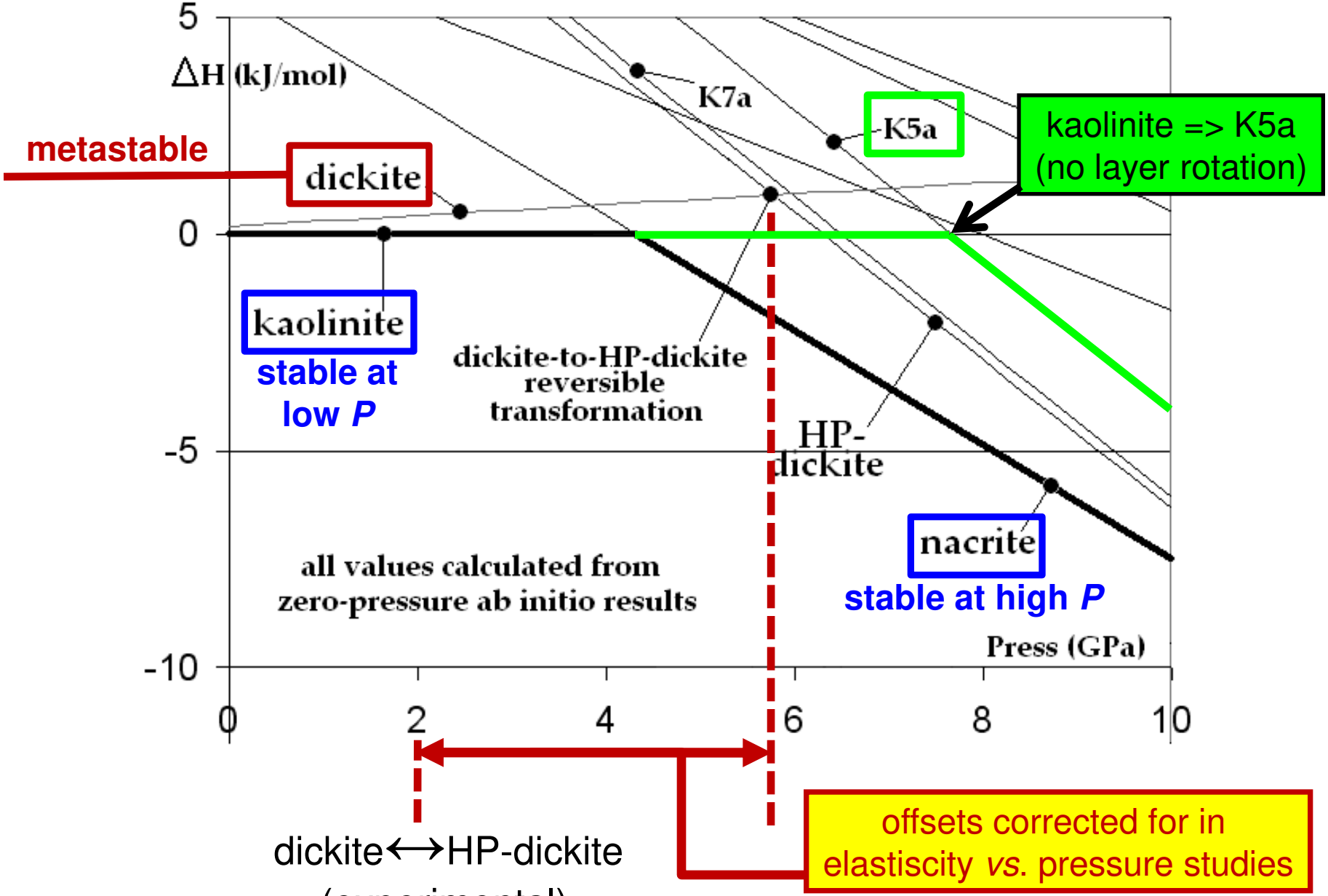

Mercier & Le Page (2008)

Experimental measurements of free energy

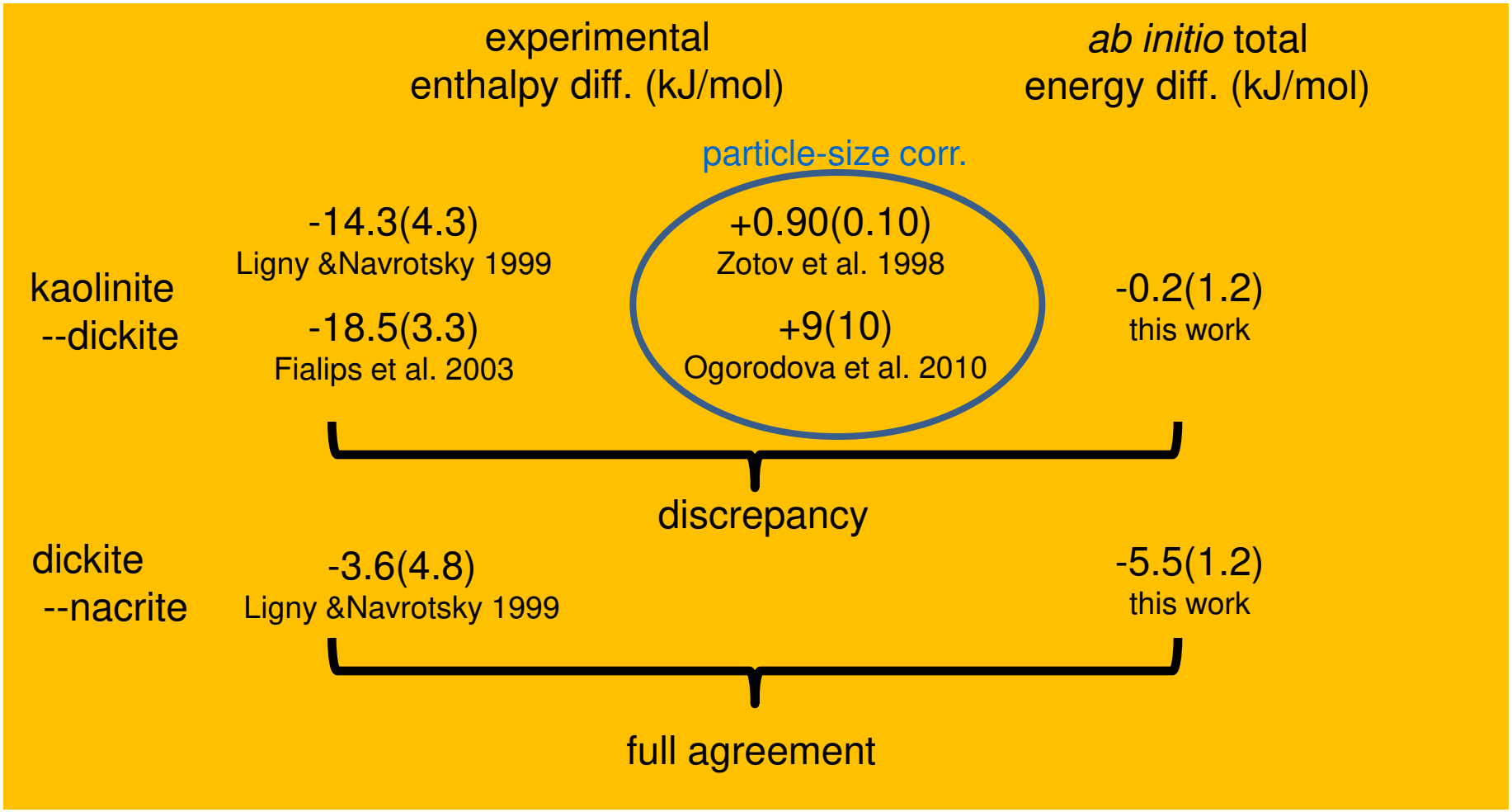

Experimental measurement of the free energy difference between kaolinite and dickite is far from settled!

Mercier & Le Page (2008) *Acta Cryst. B* 64: 131-143

$\Delta H(P, T = 0\text{K})$

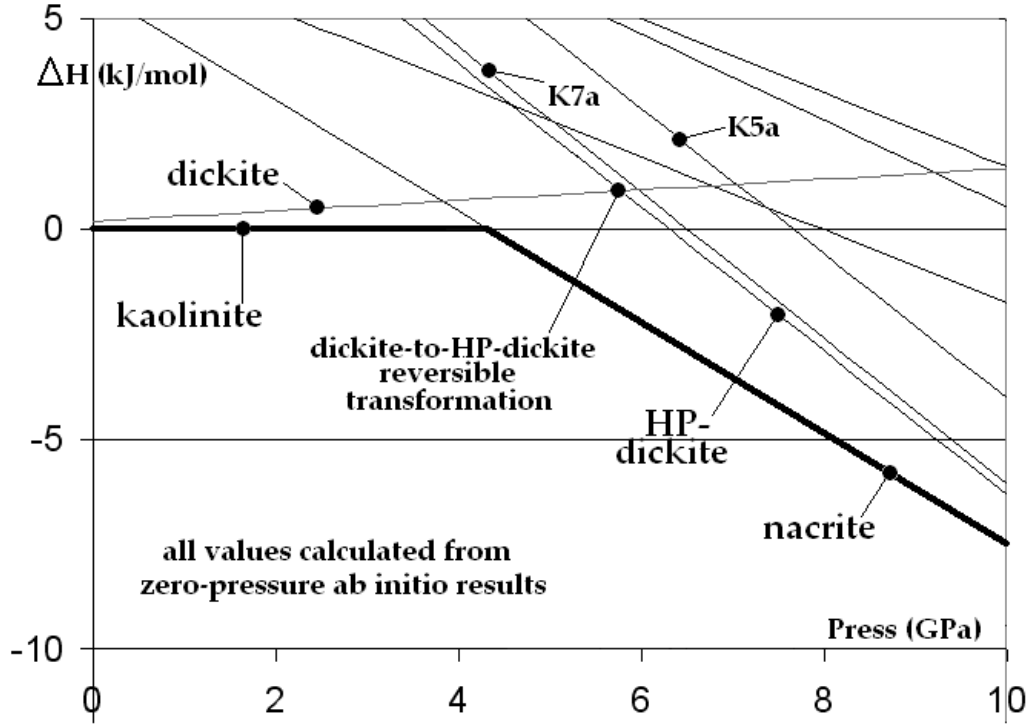

$\Delta H(P, T = T_o)$

For T ≠ 0K, the lines on the ΔH *vs.* ΔP diagram will be parallel because:

$$\Delta H = \Delta U + P\Delta V$$
$$= \Delta U + P\,[\Delta V(\text{T=0K}) + \Delta V(\text{T})\,]$$

it depends on the volume thermal expansion difference, which is expected to be both very tiny and similar from polytype to polytype

$\Delta H(P, T = 300\text{K})$

dickite↔HP-dickite
exp. phase transition

This diagram derives from the T=0K diagram by two assumptions:

(1) a correction for a 2GPa bias in all calculated P

(2) a shift to the left by 5 MPa K^{-1} for the line about HP-dickite

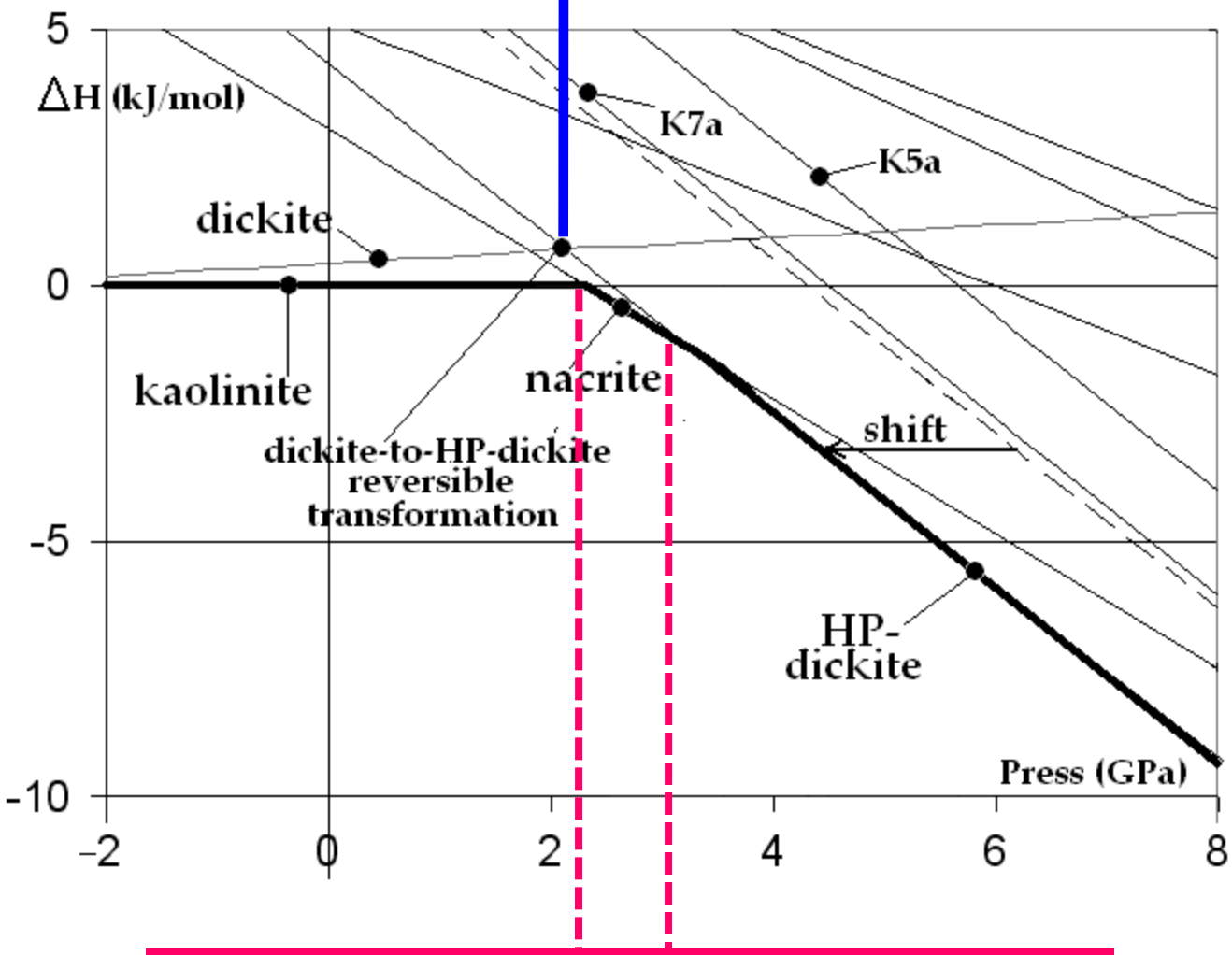

narrow stability range for nacrite wedged between kaolinite at low P and HP-dickite at high P

Mercier & Le Page (2008)
Acta Cryst. B 64: 131-143

$\Delta H(P, T = 600\text{K})$

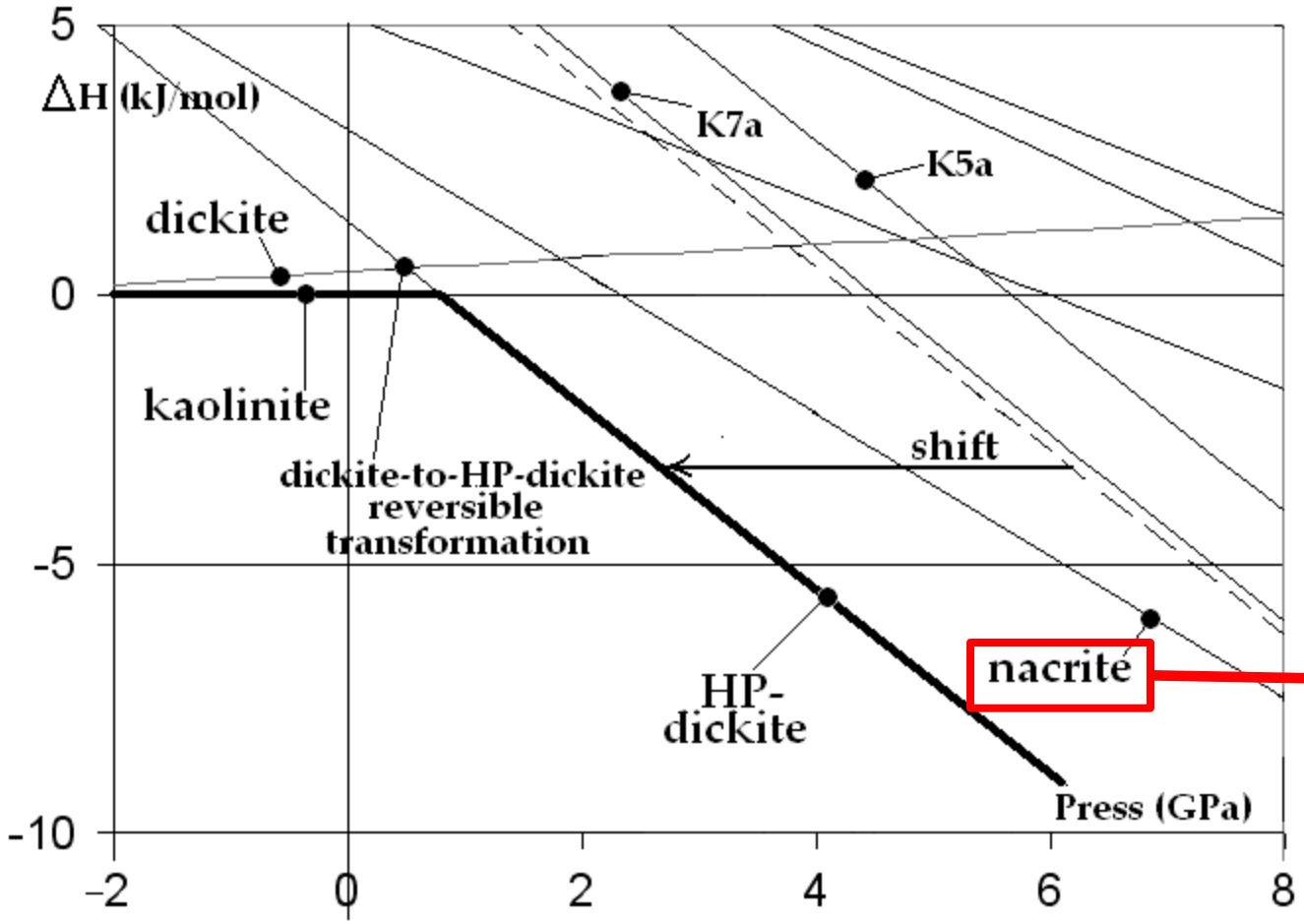

no more stability range for nacrite at T > ~450K

Mercier & Le Page (2008) *Acta Cryst. B* 64: 131-143

Diagenesis of kaolin minerals

No direct solid-state transformation of kaolinite into dickite or nacrite occurs at any point in the process.

⇒The kaolinite↔dickite and kaolinite↔nacrite transformations involve layer-layer rotations and would require reconstruction of kaolin layers.

Kaolinite, nacrite and HP-dickite crystallize in the pores of sandstones according to their respective thermodynamic domain of stability.

HP-dickite transforms reversibly into dickite via a solid-state reaction around 2 GPa. The phase observed in the laboratory is therefore dickite, which is metastable at ambient conditions, whereas the phase that formed *in situ* is HP-dickite.

Nacrite forms at pressure and temperature combinations not found with normal geothermal gradient.

Mercier & Le Page (2008) *Acta Cryst. B* 64: 131-143

We have explained

- Existence of the four known kaolin polytypes
- Diagenetic sequence and coexistence of kaolin minerals
- Role of HP-dickite in diagenetic sequence
- Stacking defects observed in kaolinite (Bookin et al. 1989)

Not Explained

- Non-observation of additional kaolin polytypes
  (They might synthesize, but at zero pressure only.)

Question marks raised
(more experimental work needed)

- High *P-T* transformations of kaolinite↔nacrite↔dickite
- Experimental free energy value of kaolinite

Dera et al. (2003) Am. Min. 88: 1426-1435

dickite ⇔ HP-dickite at ~ 2GPa

"Layer-shift phase transition does not provide a method of interconversion between the polytypes that differ by rotation of 1:1 layers"

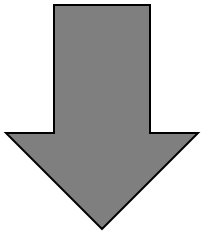

Polytype transformations involving rotation of layers, like

kaolinite ⇨ dickite or dickite ⇨ nacrite

must occur through dissolution/recrystallization or reconstructive solid-solid mechanisms

Ab initio compression of kaolinite at 0K

Mercier & Le Page (2009)
Mat. Sc. & Tech. 25: 437-442

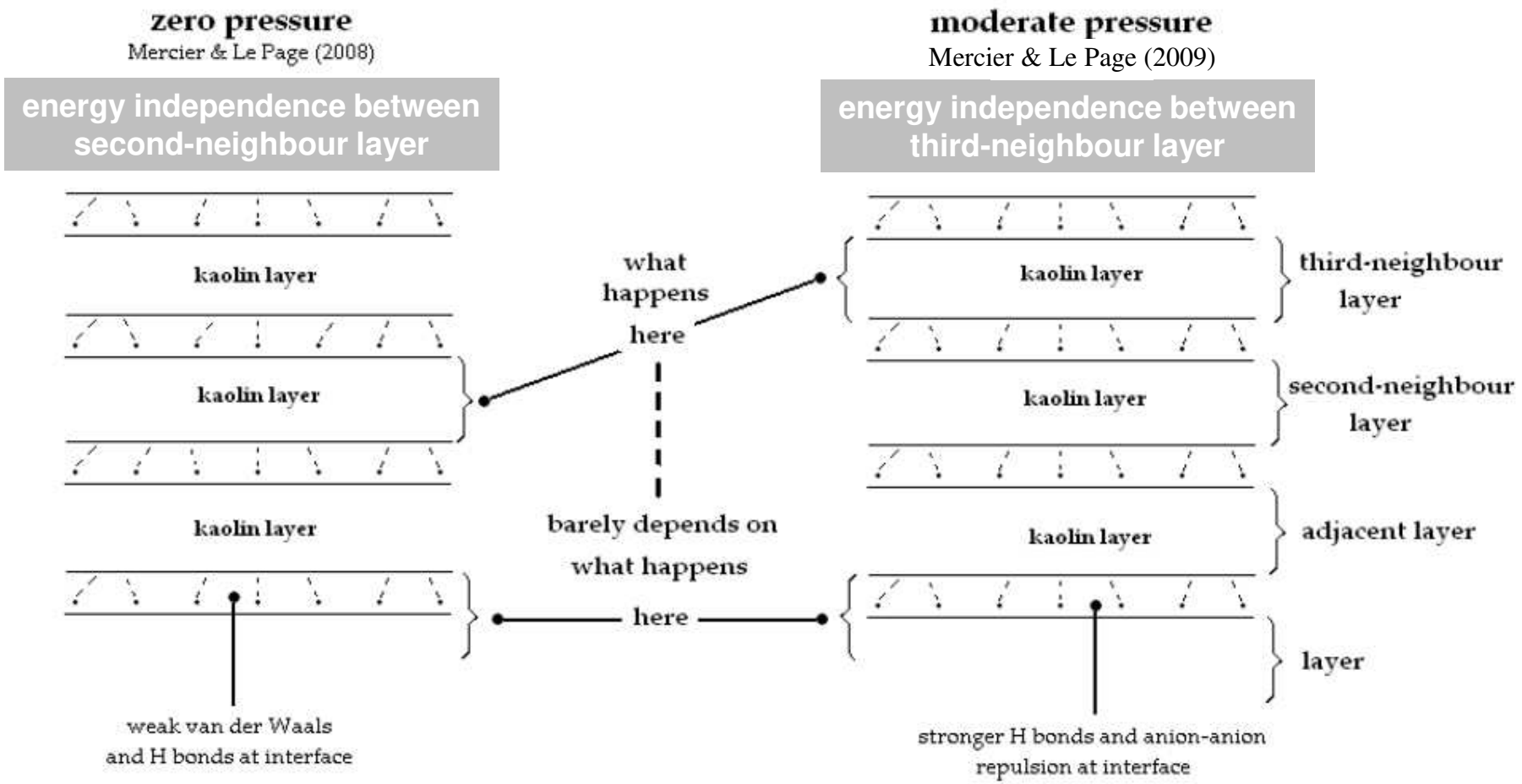

$U_{tot} = U_{layer} + \Delta A + \Delta B + \Delta C + \ldots$

stacking of single layers

$U_{tot} = U([A:B], [C:D], \ldots) = \langle U \rangle + \Delta[B:C] + \Delta[D:E] + \ldots$

stacking of pre-assembled *pairs of layers*

Table 1 The 19 possible low enthalpy models for reversible displacive transformations of kaolinite under pressure derived here. These models were derived under the assumption that contributions from third-neighbour layers and beyond to differences in total energy can be neglected

Model #	Symbol	1→2	2→3	3→4	4→1	Space group	Z
1	[KT0]a	0				*Cm*	2
2	[KT1]a	$\frac{(2a+b)}{3}$				*P*1	1
3	[KT1]b	$\frac{(2a+b)}{3}$	$\frac{(a+2b)}{3}$			*Cc*	4
4	[KT2]a	$\frac{a}{3}$				*P*1	1
5	[KT2]b	$\frac{a}{3}$	$\frac{b}{3}$			*Cc*	4
6	[KT3]a	$\frac{2(a+b)}{3}$				*Cm*	2
7	[KT1:KT0]a	$\frac{(2a+b)}{3}$	0			*P*1	2
8	[KT1:KT0]b	$\frac{(2a+b)}{3}$	0	$\frac{(a+2b)}{3}$	0	*Cc*	8
9	[KT2:KT0]a	$\frac{a}{3}$	0			*P*1	2
10	[KT2:KT0]b	$\frac{a}{3}$	0	$\frac{b}{3}$	0	*Cc*	8
11	[KT2:KT1]a	$\frac{a}{3}$	$\frac{(2a+b)}{3}$			*P*1	2
12	[KT2:KT1]b	$\frac{a}{3}$	$\frac{(2a+b)}{3}$	$\frac{b}{3}$	$\frac{(a+2b)}{3}$	*Cc*	8
13	[KT2:KT1*]a	$\frac{a}{3}$	$\frac{(a+2b)}{3}$			*P*1	2
14	[KT2:KT1*]b	$\frac{a}{3}$	$\frac{(a+2b)}{3}$	$\frac{b}{3}$	$\frac{(2a+b)}{3}$	*Cc*	8
15	[KT3:KT0]a	$\frac{2(a+b)}{3}$	0			*Cm*	4
16	[KT3:KT1]a	$\frac{2(a+b)}{3}$	$\frac{(2a+b)}{3}$			*P*1	2
17	[KT3:KT1]b	$\frac{2(a+b)}{3}$	$\frac{(2a+b)}{3}$	$\frac{2(a+b)}{3}$	$\frac{(a+2b)}{3}$	*Cc*	8
18	[KT3:KT2]a	$\frac{2(a+b)}{3}$	$\frac{a}{3}$			*P*1	2
19	[KT3:KT2]b	$\frac{2(a+b)}{3}$	$\frac{a}{3}$	$\frac{2(a+b)}{3}$	$\frac{b}{3}$	*Cc*	8

Mercier & Le Page (2009)
Mat. Sc. & Tech. 25: 437-442

Blind
ab initio optimization
up to 60 GPa of
19 ideal models
as candidates
for low enthalpy
stackings/polytypes
under pressure

Mercier & Le Page (2009)
Mat. Sc. & Tech. 25: 437-442

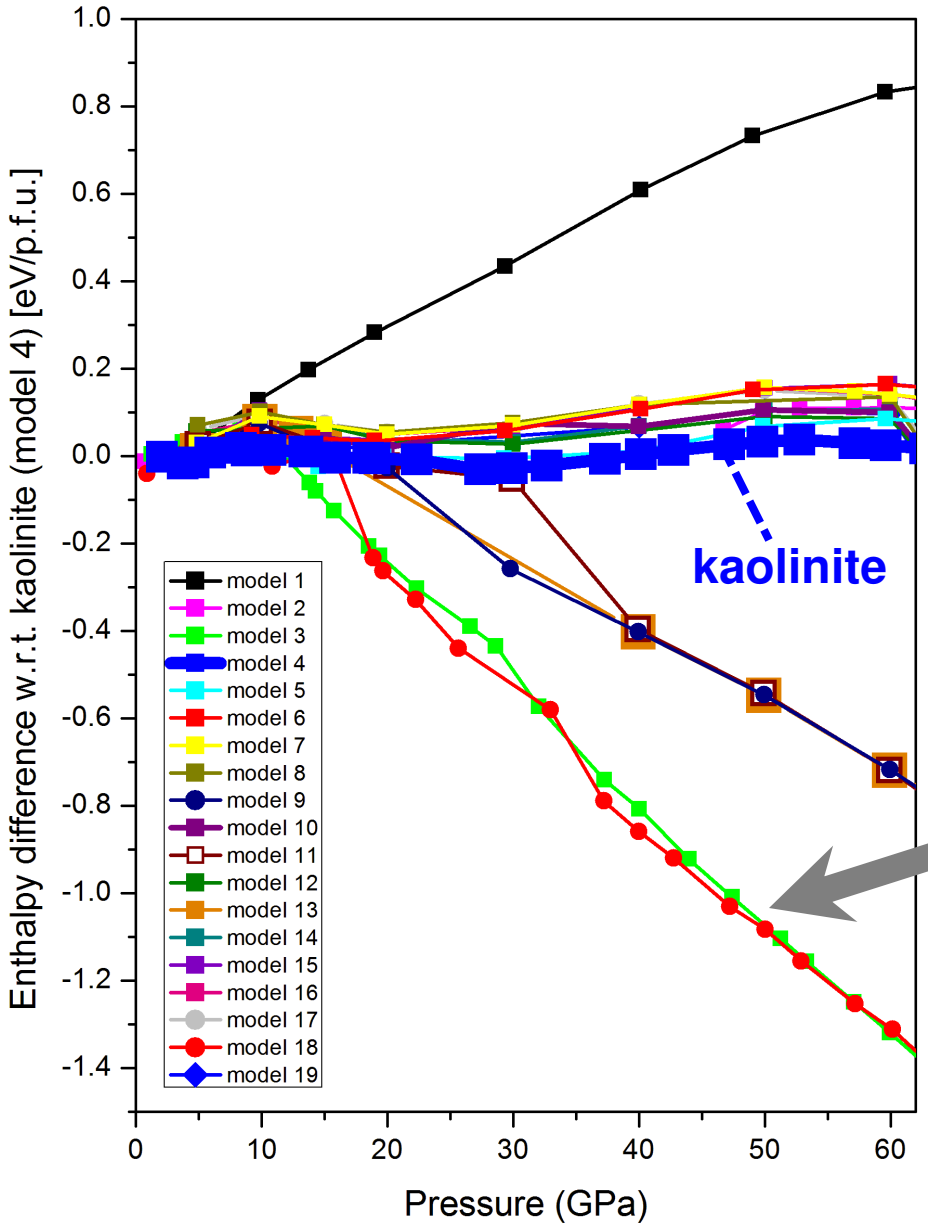

ab initio results implied that kaolinite would transform upon compression

But the two lowest enthalpy models that resulted ***accidently*** *are in fact* ***not any of the 19 stackings originally built***

Mercier & Le Page (2009)
Mat. Sc. & Tech. 25: 437-442

five-fold
silicon
coordination

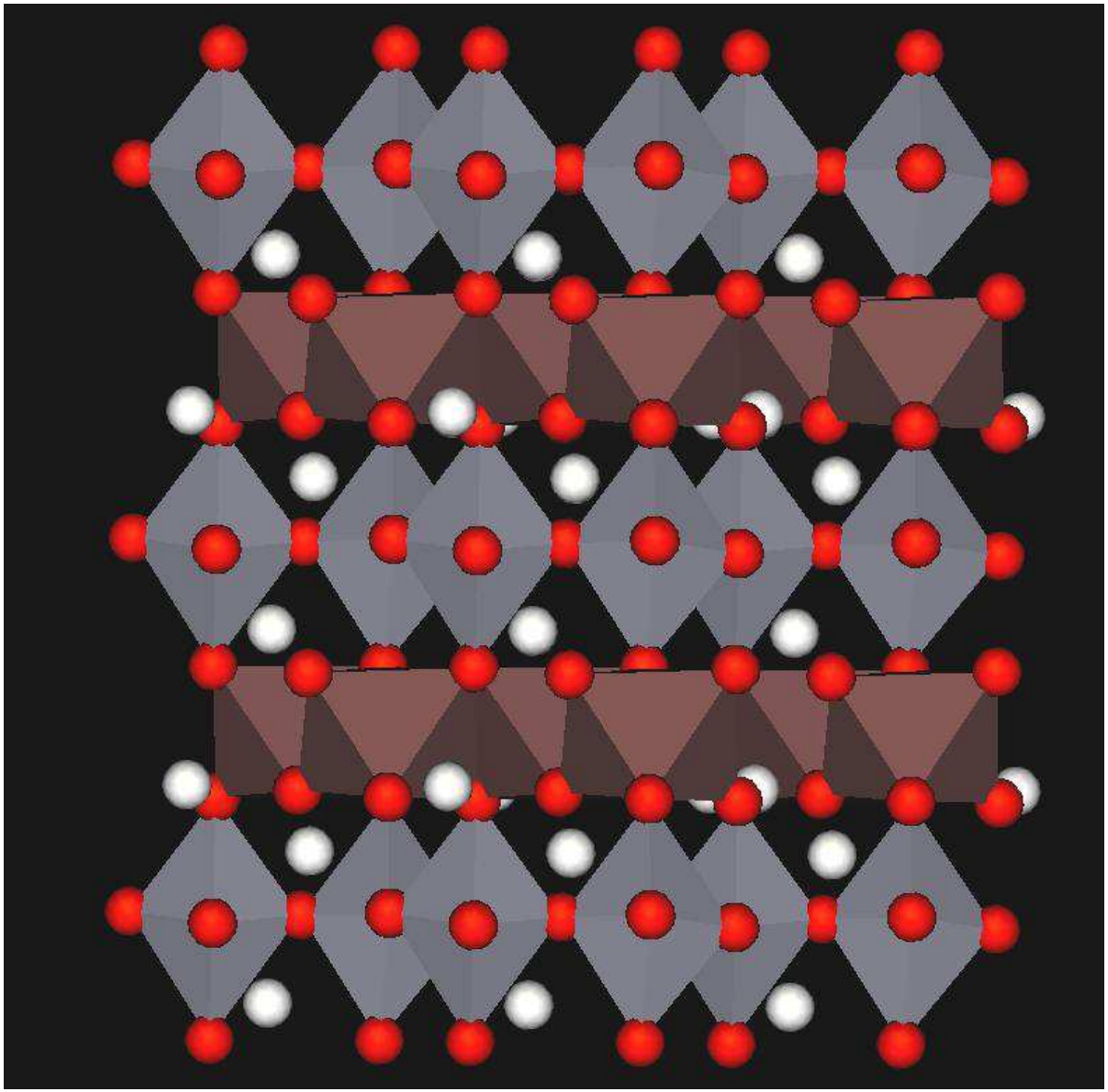

new family of
kaolin polytypes
based on
translations
not possible
at low pressure

Novel –**a**/3, –**b**/3 and (**a**+**b**)/3 translations

(not possible at low pressure)

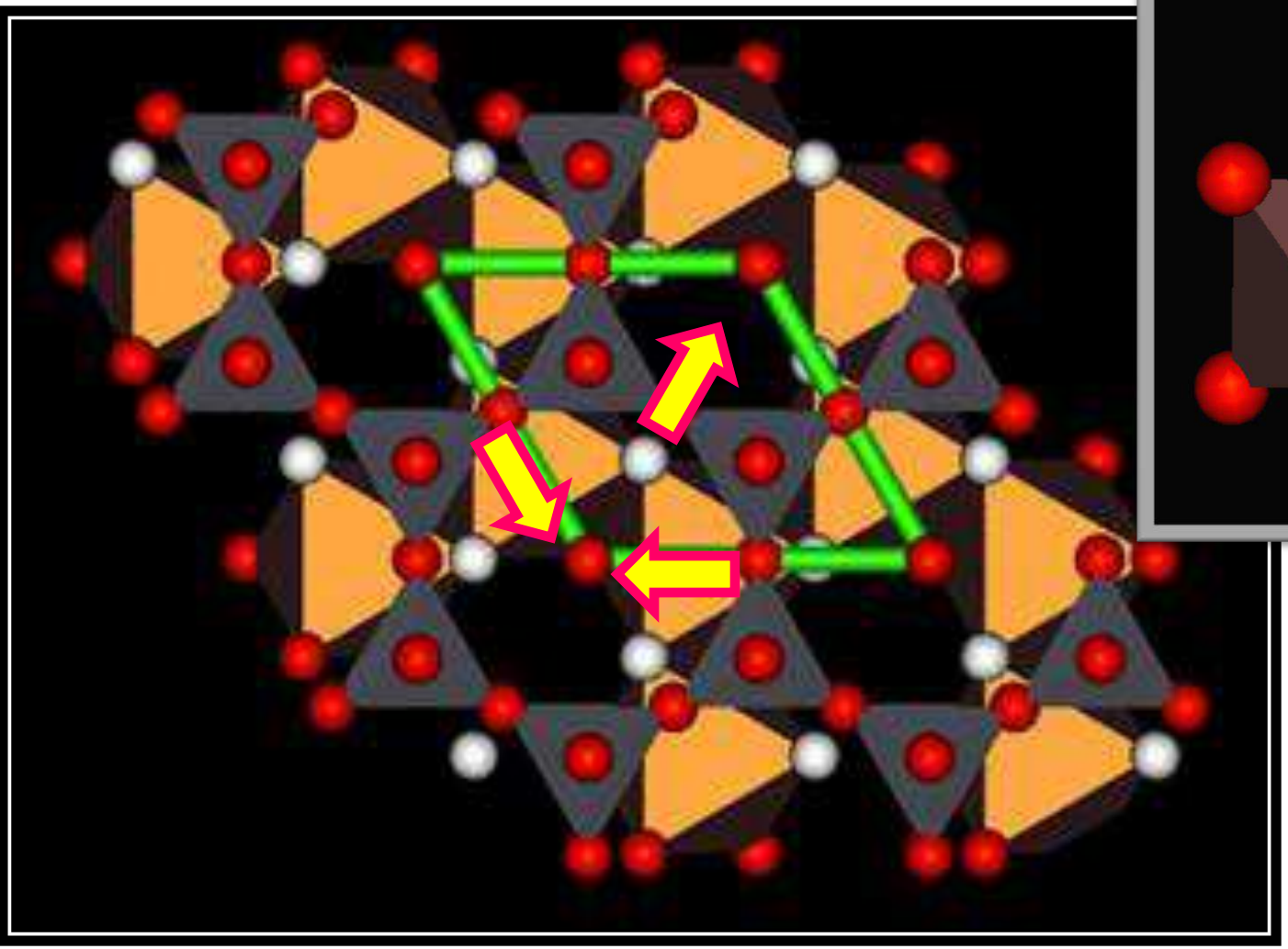

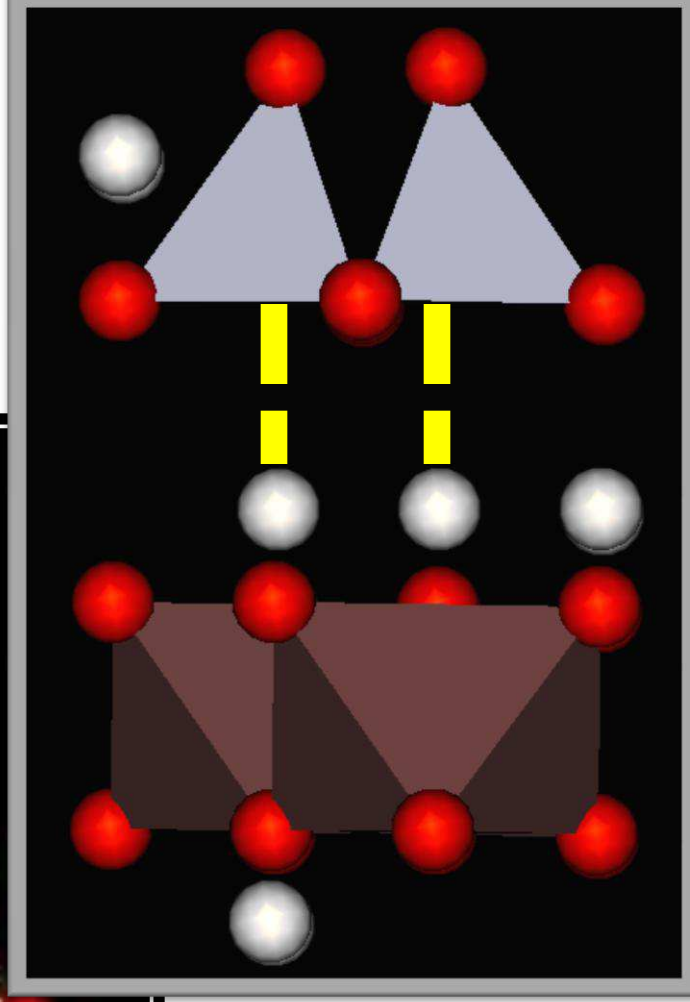

Experimental compression of Keokuk kaolinite to 7.8 GPa

Welch & Crichton (2010) Am. Min. 95: 651-654

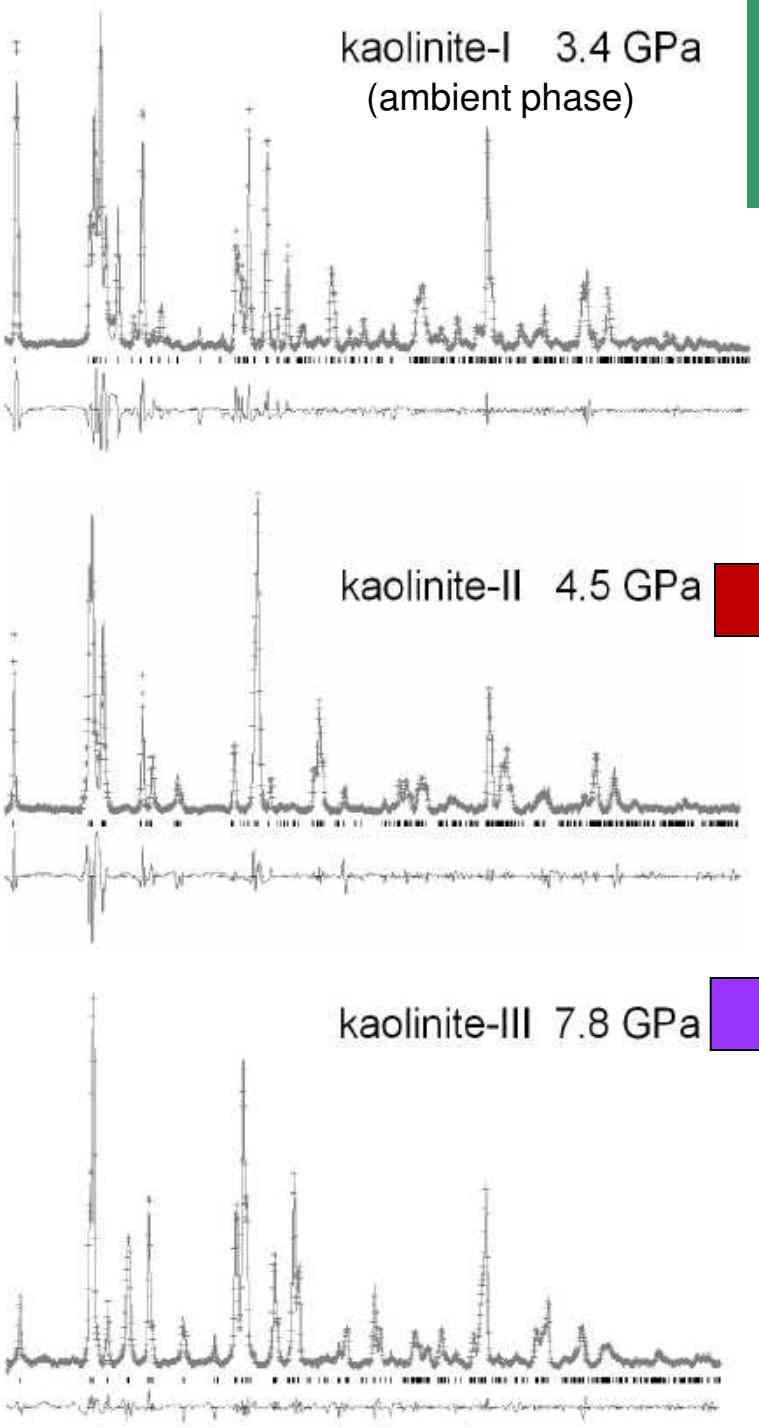

Model [K5a] (Mercier & Le Page 2008)
Model [KT1]a (Mercier & Le Page 2009)

Novel –a/3 translation predicted by Mercier & Le Page 2009

Model [KP01]a in Mercier et al. (2010) Am. Min. 95: 1117-1120
…and also more predicted phases…

More HP polytypes predicted

Mercier et al. (2010)
Am. Min. 95: 1117-1120

TABLE 1a. Repeated application of (**R**,**T**)

Translation **T**	Rotation **R**					
	0	π/3	2π/3	π	4π/3	5π/3
–**a**/3	[KP01]a	[KP11]a	[KP21]a	[KP31]a	[KP22]a*	[KP12]a*
Space group	*P*1	$P6_1$	$P3_1$	$P2_1$		
H (eV/fu)	–105.645	–105.550	–105.609	–105.659		
V/fu (Å³)	131.84	132.15	132.21	132.27		
–**b**/3	[KP01]a*	[KP12]a	[KP22]a	[KP31]a*	[KP21]a*	[KP11]a*
Space group		$P6_1$	$P3_1$			
H (eV/fu)		–105.642	–105.539			
V/fu (Å³)		132.59	132.21			
(**a**+**b**)/3	[KP03]a	[KP13]a	[KP23]a	[KP33]a	[KP23]a*	[KP13]a*
Space group	*Cm*	$P6_1$	$P3_1$	$Cmc2_1$		
H (eV/fu)	–105.576	–105.632	–105.620	–105.579		
V/fu (Å³)	131.51	132.25	132.14	131.61		

TABLE 1b. Repeated application of the sequence [(**R**,**T**):(**R***,**T***)]

Translation **T**	Rotation **R**					
	0	π/3	2π/3	π	4π/3	5π/3
–**a**/3	[KP01]b	[KP11]b	[KP21]b	[KP31]b	=[KP22]b	=[KP12]b
Space group	*Cc*	*Cc*	*Cc*	*Cc*		
H (eV/fu)	–105.608	–105.557	–105.622	–105.636		
V/fu (Å³)	131.88	132.10	131.62	132.38		
–**b**/3	=[KP01]b	[KP12]b	[KP22]b	=[KP31]b	=[KP21]b	=[KP11]b
Space group		*Cc*	*Cc*			
H (eV/fu)		–105.633	–105.535			
V/fu (Å³)		131.93	131.84			
(**a**+**b**)/3	=[KP03]a	[KP13]b	[KP23]b	=[KP33]a	=[KP23]b	=[KP13]b
Space group	*Cm*	*Cc*	*Cc*	$Cmc2_1$		
H (eV/fu)	–105.576	–105.648	–105.624	–105.579		
V/fu (Å³)	131.51	132.24	131.76	131.62		

kaolinite-IV

nacrite-II

dickite-III

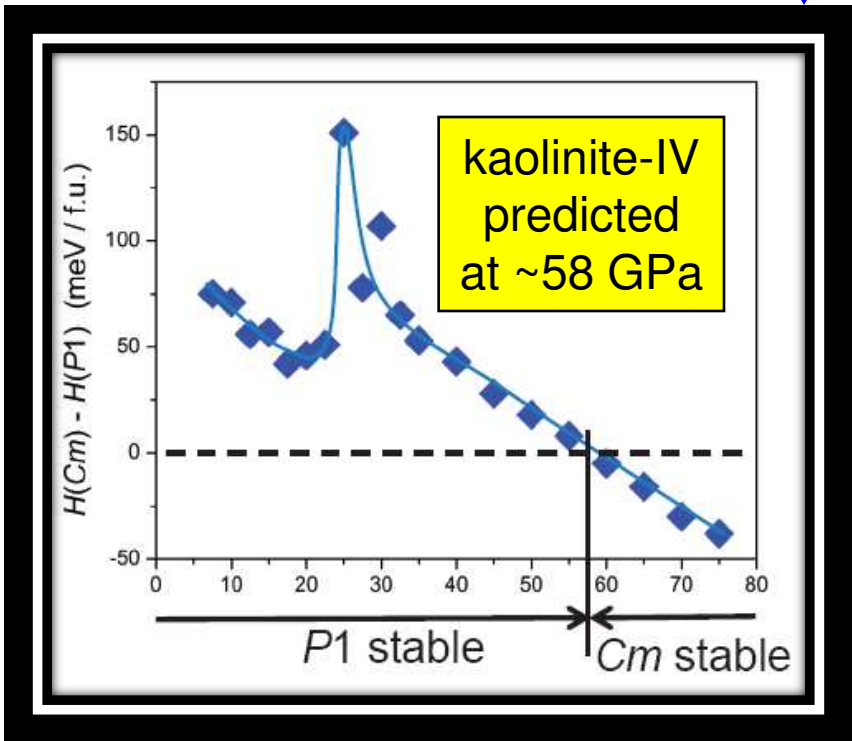

SUMMARY

From assumed energy independence of non-adjacent kaolin layers we have:

- shown that only 36 crystalline stackings could have lowest energy
- built idealized models for them and optimized them ab initio

MLP08

From this optimization, we have:

- rationalized the existence of the four known kaolin polymorphs
- proposed H/P/T graphs explaining known facts about kaolin system
- exposed as inconsistent an experimental measurement of free energy

MLP08

- predicted a new family of phases for compression of kaolinite — MLP09
- that family has subsequently been observed independently — WC10
- predicted a further phase transformation in kaolinite — MLPD10
- predicted structures that dickite-III and nacrite-II might adopt upon compression

Concluding remarks

Complementarity of experiment and *ab initio* modeling

Disparate experimental facts about a crystal-chemical system of materials allow no further scientific deduction

***Ab initio* modeling:**

- **helps to rationalize the crystal chemistry of the materials system**
- **proposes explanations for the phase changes observed in the system**
- **predicts verifiable facts and exposes dubious concepts**

MLP11

we are back here, after one full turn around the loop

MLP08

MLP09

MLPD10

until everything makes sense

WC10

kaolin system

New experimental facts, explained or not

Acknowledgements:

Partial financial support for this work was provided by the Canadian government Program of Energy and Development (PERD) and the Clean Energy Fund managed by Natural Resources Canada.